OXFORD

molecular
human
reproduction

Ovarian stimulation with excessive FSH doses causes cumulus cell and oocyte dysfunction in small ovarian reserve heifers

Kaitlin R. Karl [1], Peter Z. Schall[1,4], Zaramasina L. Clark[1,5], Meghan L. Ruebel[1,6], Jose Cibelli[1,2], Robert J. Tempelman[1], Keith E. Latham [1,3], and James J. Ireland [1,*]

[1]Department of Animal Science, Reproductive and Developmental Sciences Program, Michigan State University, East Lansing, MI, USA
[2]Department of Large Animal Clinical Sciences, Michigan State University, East Lansing, MI, USA
[3]Department of Obstetrics, Gynecology and Reproductive Science, Michigan State University, East Lansing, MI, USA
[4]Present address: University of Michigan, Ann Arbor, MI, USA.
[5]Present address: School of Biological Sciences, Victoria University of Wellington, Wellington, New Zealand.
[6]Present address: USDA-ARS, Southeast Area, Arkansas Children's Nutrition Center, Little Rock, AR, USA.

*Correspondence address. Molecular Reproductive Endocrinology Laboratory, Department of Animal Science, Michigan State University, East Lansing, MI 48824, USA. Tel: +1-517-290-7074; E-mail: ireland@msu.edu https://orcid.org/0000-0002-5923-8000

Abstract

Excessive FSH doses during ovarian stimulation in the small ovarian reserve heifer (SORH) cause premature cumulus expansion and follicular hyperstimulation dysgenesis (FHD) in nearly all ovulatory-size follicles with predicted disruptions in cell-signaling pathways in cumulus cells and oocytes (before ovulatory hCG stimulation). These observations support the hypothesis that excessive FSH dysregulates cumulus cell function and oocyte maturation. To test this hypothesis, we determined whether excessive FSH-induced differentially expressed genes (DEGs) in cumulus cells identified in our previously published transcriptome analysis were altered independent of extreme phenotypic differences observed amongst ovulatory-size follicles, and assessed predicted roles of these DEGs in cumulus and oocyte biology. We also determined if excessive FSH alters cumulus cell morphology, and oocyte nuclear maturation before (premature) or after an ovulatory hCG stimulus or during IVM. Excessive FSH doses increased expression of 17 cumulus DEGs with known roles in cumulus cell and oocyte functions (responsiveness to gonadotrophins, survival, expansion, and oocyte maturation). Excessive FSH also induced premature cumulus expansion and oocyte maturation but inhibited cumulus expansion and oocyte maturation post-hCG and diminished the ability of oocytes with prematurely expanded cumulus cells to undergo IVF or nuclear maturation during IVM. Ovarian stimulation with excessive FSH is concluded to disrupt cumulus cell and oocyte functions by inducing premature cumulus expansion and dysregulating oocyte maturation without an ovulatory hCG stimulus yielding poor-quality cumulus–oocyte complexes that may be incorrectly judged morphologically as suitable for IVF during ART.

Keywords: small ovarian reserve / excessive FSH / superovulation / oocyte retrieval / cumulus–oocyte complexes / dysregulation of cumulus function / FSH target genes in cumulus cells / premature cumulus expansion / resumption of meiosis

Introduction

Diagnosis of a small ovarian reserve (total number of morphologically healthy follicles/oocytes in ovaries) is the primary reason women seek ART (Centers for Disease Control and Prevention ASfRM, Society for Assisted Reproductive Technology, 2013). However, many women with small ovarian reserves respond poorly to treatments with FSH during ovarian stimulation protocols (Ireland *et al.*, 2011; Baker *et al.*, 2015; Clark *et al.*, 2021). Moreover, total FSH doses during ovarian stimulation protocols vary from <1000 to 20 000 IU (Baker *et al.*, 2015; Clark *et al.*, 2021), and high FSH doses during ovarian stimulation are inversely linked to ovarian function, oocyte recovery, and live birth rate during ART in women (Edwards *et al.*, 1996; Hazekamp *et al.*, 2000; Inge *et al.*, 2005; Klinkert *et al.*, 2005; Kovalevsky and Patrizio 2005; Pal *et al.*, 2008; Sterrenburg *et al.*, 2011; Baker *et al.*, 2015; Clark *et al.*, 2021) and ovarian function and embryo transfer outcomes in cattle (Greve *et al.*, 1979; Donaldson and Perry 1983; Donaldson 1984; McGowan *et al.*, 1985; Pawlyshyn *et al.*, 1986; Saumande and Chupin 1986; Sugano and Watanabe 1997). Whether excessive FSH doses during ovarian stimulation cause or contribute to poor ART outcomes, and the mechanisms responsible for such an effect, are unknown.

To better understand the impact of high FSH doses during ovarian stimulation on ovulatory follicle function, oocyte quality, and associated mechanisms, we developed the small ovarian reserve heifer (SORH) model. This unique model has biomedical relevance because it exhibits not only a relatively low number of morphologically healthy oocytes and a low antral follicle count (AFC) (Ireland *et al.*, 2007) but diminished circulating concentrations of anti-Müllerian hormone (Ireland *et al.*, 2008), progesterone and estradiol, hypersecretion of FSH (Abdalla and Thum 2004; Burns *et al.*, 2005; Ireland *et al.*, 2007) during reproductive cycles, and poor responsiveness to superovulation (Ireland *et al.*, 2007), like women with a small ovarian reserve.

Although recombinant FSH is not available for use in cattle, ovarian stimulation of the SORH model with different doses of Folltropin-V, a commercial FSH-enriched porcine pituitary preparation (cpFSH) with minimal LH contamination (<1%), has provided new insights into the potential detrimental impact of high FSH doses on ovulatory follicle function. For example, we established that cpFSH doses only 3-fold higher than the industry standard are excessive and thus economically wasteful because they do not increase number or size of ovulatory-size follicles compared with lower doses (Karl *et al.*, 2021). In addition, excessive cpFSH (Ex-cpFSH) doses are detrimental to ovulatory follicle function because they decrease both circulating estradiol concentrations and responsiveness of ovulatory-size follicles to hCG, thereby reducing ovulation rate (Karl *et al.*, 2021).

Using the SORH model, we also established that ovarian stimulation with the Ex-cpFSH doses results in premature cumulus cell expansion and luteinization (as measured by low intrafollicular estradiol but high progesterone and oxytocin concentrations) prior to an ovulatory hCG stimulus in a large proportion of the ovulatory-size follicles (Clark *et al.*, 2022a). Furthermore, based on whole transcriptome analysis data, we concluded that Ex-cpFSH doses during ovarian stimulation cause follicular hyperstimulation dysgenesis (FHD) in all ovulatory-size follicles (Clark *et al.*, 2022b). Severe abnormalities in multiple cell-signaling pathways in granulosa and cumulus cells and oocytes critical for folliculogenesis, steroidogenesis, luteinization, cell survival, ovulation, and oocyte maturation and quality characterize this disorder. Consequently, although the precise mechanisms remain unclear, FHD likely causes or contributes to the inhibition of ovulatory-size follicle growth, reduction in estradiol production, promotion of premature cumulus expansion and luteinization, and diminution of ovulation rate in response to hCG, as we observed during ovarian stimulation of the SORH model with Ex-cpFSH (Karl *et al.*, 2021; Clark *et al.*, 2022a,b). Our observations support the hypothesis that Ex-cpFSH doses during ovarian stimulation dysregulate cumulus function and oocyte maturation.

We tested our hypothesis here using the SORH model in two ways. First, we determined if Ex-cpFSH doses during ovarian stimulation resulted in dysregulation of cumulus cell genes critical for function and regulation of oocyte maturation. This was accomplished by manually interrogating our published whole transcriptome data set to determine whether any of the previously identified Ex-cpFSH-induced cumulus cell differentially expressed genes (DEGs) (Clark *et al.*, 2022b) are altered in all ovulatory-size follicles independent of individual follicular phenotypic differences, and whether these DEGs have known roles in cumulus cell function and oocyte maturation. We reasoned that cpFSH-induced overexpression of cumulus genes in all ovulatory-size follicles could explain the premature cumulus expansion observed in nearly all ovulatory-size follicles developing in response to Ex-cpFSH doses in our studies (Clark *et al.*, 2022a,b). Second, we tested whether the Ex-cpFSH-induced premature cumulus expansion observed in our studies (Clark *et al.*, 2022a,b) is accompanied by altered oocyte nuclear maturation before (premature) or after an ovulatory hCG stimulus, or during IVM.

Materials and methods
Analysis of Ex-cpFSH-induced differentially expressed cumulus genes and their predicted roles in regulating cumulus cell function and oocyte maturation

In our previously published study (Clark *et al.*, 2022b), we analyzed by RNA sequencing four ovulatory-size follicle Types that had been identified based on FSH dose, cumulus–oocyte complex (COC) morphology (expanded, compact), and differences in intra-follicular concentrations of estradiol, progesterone and oxytocin (Clark *et al.*, 2022b). Type 1 ovulatory-size follicles were those from animals receiving the industry standard dose and mimic healthy ovulatory follicles during estrous cycles in cattle (Ireland and Roche 1982, 1983), having compact COCs (comCOCs), higher intrafollicular estradiol than progesterone concentrations, and relatively low oxytocin concentrations (Clark *et al.*, 2022a,b). Types 2, 3, and 4 follicles were identified in Ex-cpFSH treated SORH (Clark *et al.*, 2022a,b). Type 2 phenotypically resembles Type 1. Type 3 is like Type 1 and 2 but has an expanded layer of cumulus cells (expCOCs). Type 4 also has expCOCs but has much higher progesterone than estradiol and the highest oxytocin concentrations. Through RNA sequencing, we identified 4576 DEGs (characteristic of the FHD phenotype) in granulosa and cumulus cells and oocytes of the Ex-cpFSH-induced Type 2, 3, or 4 compared with the industry-standard cpFSH-induced Type 1 (control) ovulatory-size follicles. Of these 4576 DEGs, 3288 were observed in cumulus cells of the Type 2, 3, or 4 ovulatory-size follicles (Clark *et al.*, 2022b). In the present study (Fig. 1A), we manually interrogated each of these cumulus cell DEGs to identify those that were common to all three Ex-cpFSH ovulatory-size follicle types (Type 2, 3, and 4) and determined, based on a literature search, whether these DEGs have known roles in regulation of cumulus function and oocyte maturation (Fig. 1A).

Effect of Ex-cpFSH on cumulus expansion and oocyte maturation

We conducted three experiments using the SORH model (Fig. 1B). The first experiment (Exp 1, Fig. 1B) determined whether Ex-cpFSH doses during ovarian stimulation altered cumulus morphology and stage or timing of oocyte nuclear maturation. Each ovulatory-size ($\geq$10 mm in diameter) follicle for each heifer (n = 10) was subjected to oocyte retrieval 12 h after the last cpFSH dose (*no hCG stimulus given*) and each COC was classified morphologically as comCOCs or expCOCs, and stage of nuclear maturation attained for oocytes within each COC was determined. Exp 2 (Fig. 1B) determined whether Ex-cpFSH treatment during ovarian stimulation altered the capacity of cumulus cells and oocytes in ovulatory-size follicles to respond to an ovulatory hCG stimulus. Heifers were injected with an ovulatory dose of hCG 12 h after the last cpFSH injection. Each ovulatory-size follicle for each heifer (n = 16) was subjected to oocyte retrieval 24 h post-hCG but prior to ovulation. The responsiveness of cumulus cells and oocytes to the ovulatory hCG stimulus was then evaluated by morphological classification of each COC as comCOCs or expCOCs, and determination of nuclear maturation stage attained for the oocyte within each COC. Exp 3 (Fig. 1B) determined if the Ex-cpFSH doses during ovarian stimulation altered the capacity of expCOCs to resume meiosis during IVM and their ability to be fertilized by IVF. Each ovulatory-size follicle for each heifer (n = 18) was subjected to oocyte retrieval 12 h after the last cpFSH (*no ovulatory hCG stimulus given*) and each recovered COC was classified morphologically as comCOCs or expCOCs. The expCOCs from the Ex-cpFSH treated heifers (n = 8) were subjected to IVF and compared to comCOCs from abattoir ovaries that were also subjected to IVF. Additionally, a subset of Ex-cpFSH treated heifers (n = 10) was used to assess nuclear maturation stages of expCOCs versus comCOCs after IVM (Fig. 1B).
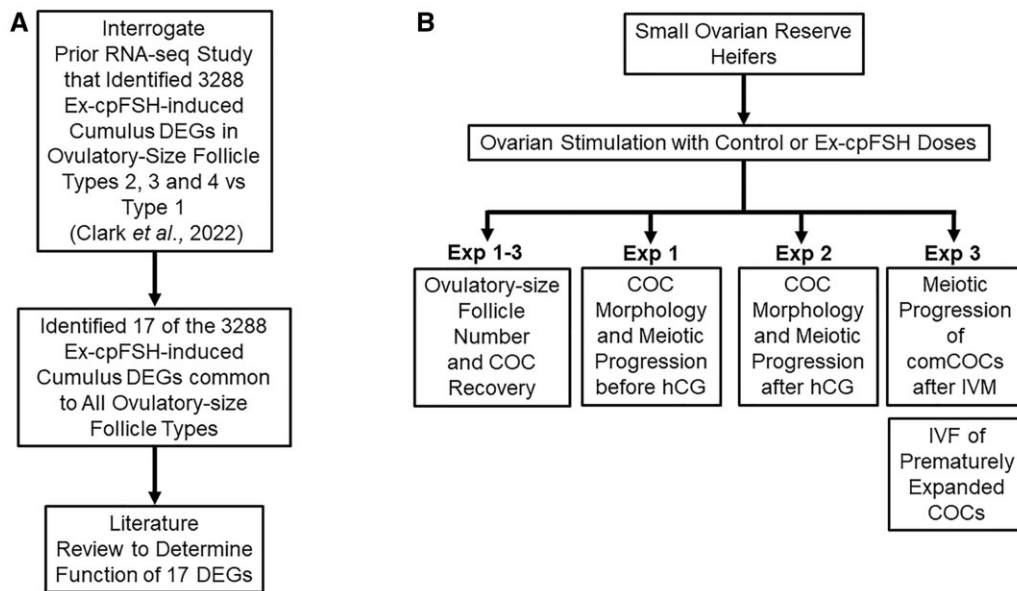
Figure 1. Experimental approaches for analysis of FSH action on cumulus cell function and oocyte maturation in the small ovarian reserve heifer. To test the hypothesis that excessive FSH action during ovarian stimulation dysregulates cumulus cell function and oocyte maturation, we determined: (**A**) if any of the 3288 Ex-cpFSH-induced cumulus DEGs in Types 2, 3, and 4 versus 1 ovulatory-size follicles of the SORH model, identified in our previously published transcriptome data set (Clark et al., 2022b), were common to all ovulatory-size follicles independent of their Type and if these DEGs were critical for cumulus function and oocyte maturation. We also determined: (**B**) if Ex-cpFSH doses during ovarian stimulation of the SORH model altered number of ovulatory-size follicles and COC recovery rate (Exp 1–3), cumulus cell morphology (Exp 1–2), nuclear maturation of oocytes before (premature, Exp 1) or after an ovulatory hCG stimulus (Exp 2) or after IVM of comCOCs (Exp 3), and IVF of prematurely expCOCs (Exp 3). Ex-cpFSH, excessive commercial FSH-enriched porcine pituitary preparation; DEGs, differentially expressed genes; SORH, small ovarian reserve heifer; COC, cumulus–oocyte complex; Exp, experiment; comCOCs, compact cumulus–oocyte complexes; expCOCs, expanded cumulus–oocyte complexes.

Reagents

Unless otherwise mentioned, chemicals and reagents were purchased from Merck KGaA (Darmstadt, Germany).

Identification of heifers with a small ovarian reserve

We previously established that 11- to 12-month-old heifers with a low AFC ($\leq$15 follicles of $\geq$3 mm in diameter) during ovarian follicular waves (15–20% of a herd) also have 80% smaller ovarian reserves (total number morphologically healthy follicles and oocytes in ovaries) compared with age-matched counterparts with a high AFC ($\geq$25 follicles) (Burns et al., 2005; Ireland et al., 2007, 2008, 2009; Jimenez-Krassel et al., 2009; Mossa et al., 2010). In the present study, serial ovarian ultrasonography was used to identify 11- to 12-month-old Holstein heifers of similar weights with a low AFC and small ovarian reserve (Karl et al., 2021) for ovarian stimulation.

Ovarian stimulation protocol

To synchronize estrous cycles for ovarian stimulation, heifers received an initial 2 ml i.m. injection of prostaglandin-$F_{2\alpha}$ (PG, 12.5 mg dinoprost/ml, Lutalyse *HighCon*, Zoetis, Parsipanny, NJ, USA) followed by two additional PG injections 12 h apart 10 days later. Each heifer underwent daily ovarian ultrasonography to detect ovulation and emergence of the first follicular wave. The first injection of Folltropin-V (porcine pituitary extract containing primarily FSH with 0.25% LH contamination (cpFSH), Vetoquinol USA Inc., Fort Worth, TX, USA) began 36 h after the last PG injection which was $\pm$1 day from ovulation and initiation of the first follicular wave in all heifers. Heifers received 8 i.m. injections of cpFSH (either 70 IU or 210 IU) at 12-h intervals. The cpFSH dose range per injection was 20% lower and 240% higher than the Vetoquinol recommended dose per injection of 87.5 IU. Hereafter,

the 70 IU industry-standard cpFSH dose is referred to as the control while the 210 IU cpFSH is referred to as the Ex-cpFSH dose. Following superovulation, either two or three i.m. PG injections were given 12 h apart starting at the time of the seventh cpFSH injection (about Day 4 or 5 of the estrous cycle) to regress the newly formed corpus luteum during each ovarian stimulation regimen. Oocyte retrieval was then conducted 12 h after the last cpFSH and PG injections or 24 h after a single 2.5 ml (2500 IU) i.m. injection of hCG (Chorulon HCG 10 000 IU, Merck Animal Health USA, Rahway, NJ, USA) to induce oocyte maturation but prior to ovulation.

Oocyte retrieval from ovulatory-size follicles

For oocyte retrieval, heifers received caudal epidural anesthesia with lidocaine hydrochloride 2% (0.22 mg/kg; Lidocaine 2%, VetOne, Boise, ID, USA) mixed with xylazine hydrochloride 10% (0.025 mg/kg; AnaSed, VetOne) to minimize the stress of rectally manipulating ovaries for oocyte retrieval. Follicles $\geq$10 mm were aspirated using a real-time B-mode ultrasound scanner (Ibex EVO; E.I. Medical Imaging, Loveland, CO, USA) equipped with an 8.0 MHz microconvex transducer housed in a plastic vaginal probe with a stainless-steel needle guide connected to the aspiration equipment. COCs were aspirated from each follicle using an 18-gauge $\times$ 3-inch disposable follicular aspiration needle (Partnar Animal Health, Port Huron, MI, USA) connected to a Brazilian-style IVF tubing (Partnar Animal Health) and inserted into the stainless-steel needle guide. The contents of each follicle were aspirated into a 50 ml conical collection tube using an electric suction pump (K-MAR-5200, Cook Medical, Brisbane, Australia) at a variable negative pressure of 200 $\pm$ 1 mm Hg. Each 50 ml conical collection tube contained $\sim$3 ml of medium, which consisted of protein-free chemically defined hamster embryo culture medium-6 (HECM (Schramm and Al-Sharhan, 1996)) and HEPES.

The HECM–HEPES (HH) medium (Patel *et al.*, 2007) was supplemented with 0.3% bovine serum albumin (BSA), 500 µM 3-isobutyl-1-methylxanthine (IBMX), and 100 nM C-type natriuretic peptide (NPPC). IBMX and NPPC were used to block oocyte maturation (Soto-Heras *et al.*, 2019). Before each oocyte retrieval, the needle, IVF tubing, and 50 ml conical collection tubes were pre-coated with HH medium supplemented with 0.3% BSA and 5% polyvinyl propylene.

Morphological classification of COCs

To classify COCs, the contents of each 50 ml conical collection tube containing COCs were poured over an embryo filter (Hy-flow filter, SPI™, Canton, TX, USA) to isolate the COCs from each heifer. The filter was sprayed with HH medium to transfer COCs into a Petri dish. A stereomicroscope was used to classify each COC based on the number of cumulus cell layers (Yang *et al.*, 2017), as reported by us for cattle subjected to ovarian stimulation (Clark *et al.*, 2022a). comCOCs had one or more layers of cumulus cells surrounding the zona pellucida and oocyte whereas expCOCs had partially or totally expanded cumulus cells surrounding the zona pellucida and oocyte. Denuded oocytes devoid of cumulus cells were also recorded.

IVM

When comCOCs or expCOCs were subjected to IVM, they underwent four washes in drops of HH medium without IBMX and NPPC followed by four washes in the IVM medium. The IVM medium consisted of Medium 199 supplemented with 22 µg/ml sodium pyruvate, 4 IU/ml hCG (Chorulon®; Merck & Co., Inc., Rahway, NJ, USA), 50 µg/ml gentamicin, and 100 µl/ml fetal bovine serum (Patel *et al.*, 2007). COCs were cultured in 10 µl drops of IVM medium in groups of 3–5 for 22 h at 38.5°C in a 5% CO_2 atmosphere with 100% humidity.

To assess the nuclear maturation of COCs after IVM, our statistical power analysis limited us to groups of 3–5 COCs per drop from each heifer unless otherwise specified. However, a preliminary study was conducted to aspirate COCs from ovaries collected from cattle at a local abattoir (West Michigan Beef Co LLC, Hudsonville, MI, USA) to determine if 3 or 5 COCs per drop was representative of the proportion of oocytes reaching metaphase II (MII) during IVM. Chi square analysis indicated that groups of 3 (n = 55) or 5 (n = 31) COCs per drop did indeed produce similar proportions of MII oocytes during IVM (mean ± SEM, 71 ± 2% versus 80 ± 6%, respectively, $P \geq 0.85$). Data for heifers that had <3 COCs recovered by oocyte retrieval were not subjected to IVM and were omitted from statistical analysis.

IVF of expCOCs

Unless specified, all IVF media were purchased from IVF Bioscience, Cornwall, UK. The expCOCs were incubated at 5% CO_2 in air at 38.5°C in high humidity. All expCOCs were rinsed in HEPES-buffered HECM containing 1 mg/ml BSA (HH-BSA) (Seshagiri and Bavister, 1989) and placed in the incubator in a 44 µl drop of pre-equilibrated BO-IVF medium under mineral oil. Frozen sperm from a single high fertility bull (Lolo, STgenetics, Navasota, TX, USA) was thawed at 38°C for 1 min and rinsed twice in BO-SEMENPREP medium using two consecutive 4 min centrifugations at 350*g* at 22°C. After the final rinse, the sperm pellet was resuspended in BO-IVF at a final concentration of 2.0 × 10^6 sperm/ml in a 6 µl volume of the suspension, which was then added to 44 µl drops containing the expCOCs for 18 h. Subsequently, presumptive zygotes had their cumulus cells removed in 1 mg/ml hyaluronidase in HH-BSA using a 140 µm

internal diameter glass pipette. After three rinses in HH-BSA, embryos were incubated in BO-IVC medium for 7.5 days at 38.5°C.

Classification of stages of nuclear maturation

To determine nuclear maturation stages, oocytes were processed as reported (Prentice-Biensch *et al.*, 2012). The comCOCs and expCOCs were kept separate and washed three times in HH medium containing IBMX and NPPC and denuded by placing them into 2 ml microcentrifuge tubes containing 200 µl of 1% hyaluronidase solution at 37°C for 5 min followed by vortexing for 5 min. Denuded oocytes were then washed three times in HH medium containing IBMX and NPPC, transferred to four-well plates, and incubated for 15 min at room temperature in a permeabilization and fixation medium (6% Triton X-100 (v:v) in 3.7% paraformaldehyde solution (wt/vol)). The oocytes were washed three times again in Dulbecco's PBS without calcium and magnesium for 15 min at room temperature. Groups of ≤5 oocytes from comCOCs or expCOCs were transferred to 5 µl drops of VectaShield® Plus Antifade Mounting Medium with 4',6-diamidine-2'-phenylindole dihydrochloride (DAPI; Vector Laboratories®, Inc., Burlingame, CA, USA, H-2000-10) and mounted onto a glass slide under a coverslip.

Oocytes were examined under an epifluorescence microscope to determine the stage of nuclear maturation (Lodde *et al.*, 2007; Prentice-Biensch *et al.*, 2012) (Fig. 2). Oocytes with intact germinal vesicles (GV) were classified as G0, G1, G2, and G3 as depicted (Fig. 2A–D, respectively). The GV classifications were confirmed with anti-lamin A/C labeling, as reported (Prentice-Biensch *et al.*, 2012) (data not shown). The proportions of ovulatory-size follicles at the G0, G1, G2, or G3 nuclear stage were similar ($P > 0.05$) independent of cpFSH dose (data not shown), and thus combined into a single nuclear stage, hereafter called GV. All other oocytes not in the GV stage were classified as GV breakdown (GVBD), metaphase I (MI), or metaphase II (MII), as depicted (Fig. 2E–G, respectively). In addition, oocytes with no visible nuclear material or fragmented chromosomes were classified as degenerated.

Statistical analysis

The R package DSeq2 (Love *et al.*, 2014) was used in our previous transcriptome study (Clark *et al.*, 2022b) to determine that 3288 genes in cumulus cells were significantly (false discovery rate (FDR) <0.01, except where noted as FDR < 0.05 in Table 1) DEGs when Type 2, 3, and 4 ovulatory-size follicles were compared with Type 1 ovulatory-size follicles. In the present study, we manually interrogated each of these Ex-cpFSH-induced 3288 cumulus cell DEGs (Clark *et al.*, 2022a) to determine whether any of the cumulus DEGs were common to all ovulatory-size follicles independent of their individual phenotypes. For statistical comparisons where zero expression values are obtained for genes in some samples (Fig. 3), DESeq2 uses a maximum likelihood estimate to assign very small values less than one to those entries. The maximum likelihood estimate reflects the maximum likelihood of detection with a small number of additional reads counted.

We conducted three experiments (Exp) in the present study to determine if ovarian stimulation of the SORH model with Ex-cpFSH dysregulates cumulus function and oocyte nuclear maturation. Prior to data collection, a power analysis was conducted to determine the minimum number of animals and COCs per animal required to detect effects at a significance level of $P \leq 0.05$ at a power level of 0.80 using a balanced crossover design (SAS Inc. 2013). Analysis determined that a minimum of five animals per dose (10 animals total) and a minimum of three to five COCs per animal would be sufficient to meet these criteria.
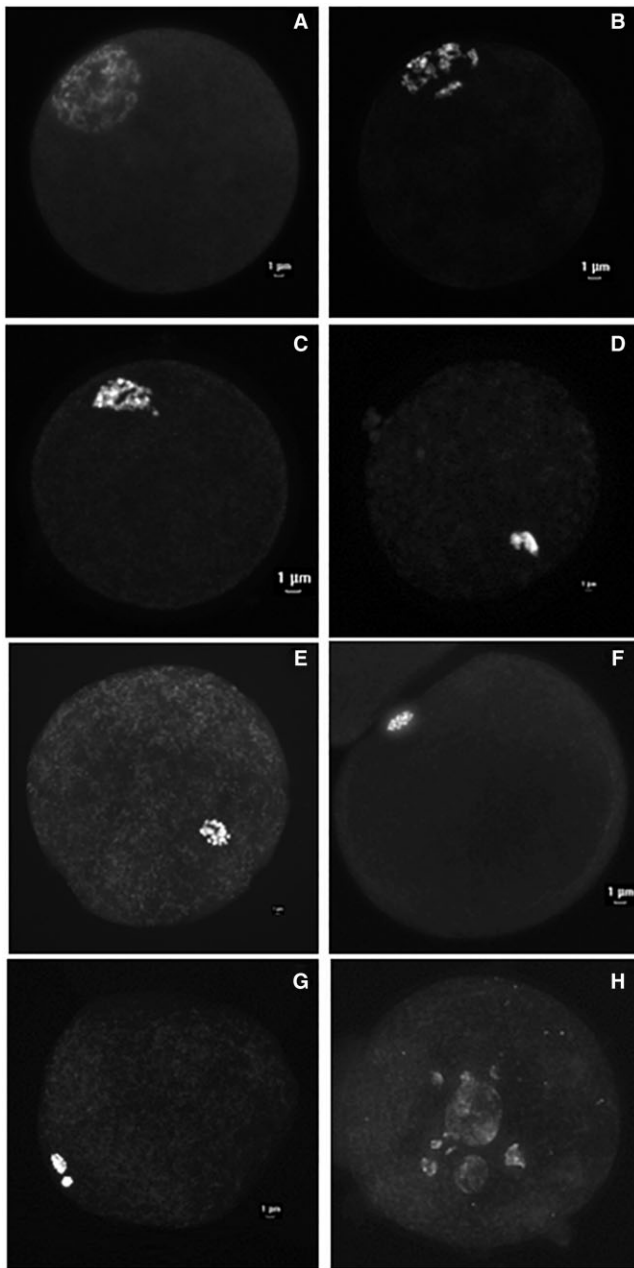
Figure 2. Representative images of the different stages of nuclear maturation of oocytes from the in the small ovarian reserve heifer. COCs were denuded, stained with DAPI and oocyte nuclear maturation stage determined as explained in Materials and Methods. The GV stages of nuclear maturation of oocytes are as follows: (**A**) GV0 = diffuse filamentous pattern of chromatin in the whole nuclear area, occasionally surrounding the nonfluorescent nucleolus; (**B**) GV1 = similar to GV0 except only a few condensed chromatin foci were detected in the nucleus; (**C**) GV2 = chromatin was further condensed into clumps, or a strand distributed throughout the nucleoplasm; or (**D**) GV3 = chromatin condensed into a single clump within the nuclear envelope. Oocytes not classified at a GV stage were classified as: (**E**) germinal vesicle breakdown = GVBD, (**F**) metaphase I = MI, (**G**) metaphase II = MII, or (**H**) degenerated = oocytes with fragmented chromosomes or without visible nuclear material. COCs, cumulus–oocyte complexes; GV, germinal vesicle.

To minimize animal numbers and confounding variables, a balanced crossover design was used. Each heifer acted as its own control, and each heifer was subjected to ovarian stimulation twice with a different cpFSH dose [70 IU (40 mg/2 ml) or 210 IU (120 mg/6 ml)] and with a different cpFSH dose sequence (e.g. 70,

210 IU versus 210, 70 IU) at the first and second ovarian stimulation regimen (Karl *et al.*, 2021). One heifer in Exp 2 was hyperresponsive to both doses of cpFSH (70 and 210 IU; 60 and 70 ovulatory-size follicles, respectively). When normality and distribution were evaluated statistically, that heifer was a statistical outlier and thus removed from further analysis (SAS Inc., 2019). In Exp 3, several heifers from each cpFSH dose group were removed from statistical analysis because oocyte retrieval resulted in <3 COCs (control, one heifer removed; Ex-cpFSH, four heifers removed), as explained above.

The responses for Exp 1–3 were expressed as binomial proportions using total number of COCs analyzed as the denominator. The model statement for logistic regression analysis included dose of cpFSH, COC morphology, oocyte nuclear stage of maturation, and the associated interaction between these variables. Estimates were reported as the mean (±SEM) proportion of ovulatory follicles per heifer with comCOCs, expCOCs or denuded oocytes, or proportion of ovulatory-size follicles per heifer with comCOCs or expCOCs at GV, GVBD, MI, MII, or with degenerated oocytes. Unless specified otherwise, all statistical analyses were performed using Statistical Analysis System (SAS 9.4 Institute, Cary, NC, USA) PROC GLIMMIX and PROC LOGISTIC (SAS Inc., 2015, 2019). When using PROC LOGISTIC, Firth's Penalized Likelihood was also used for analyzing the stages of oocyte nuclear maturation data from each Exp to mitigate nonconvergence caused by the presence of all-zero responses for a particular treatment within the dataset (Karabon, 2020). The cpFSH dose effects were considered significant if $P \leq 0.05$.

Results

Ex-cpFSH induces across all follicle phenotypes 17 DEGs that have predicted roles in regulation of cumulus cell function and oocyte maturation

This analysis of our previously published data yielded 17 shared cumulus DEGs common to Type 2, 3, and 4 ovulatory-size follicles as depicted in Volcano (Fig. 3) and Box Whisker Plots (Fig. 4). These 17 Ex-cpFSH-induced cumulus cell DEGs all have well-established roles in modulation of FSH action and cumulus cell function, including induction of cumulus cell expansion and regulation of oocyte maturation as indicated in Table 1.

Ex-cpFSH did not increase number of ovulatory-size follicles or COC recovery

The numbers of ovulatory-size follicles for each heifer were counted, and COCs were recovered 12 h after the last cpFSH injection in Exp 1, and 3 and 24 h after the ovulatory hCG stimulus in Exp 2. The number of ovulatory-size follicles, number of aspirated ovulatory-size follicles, number of COCs recovered, and COC recovery rate were similar ($P > 0.05$) between heifers treated with the different cpFSH doses (Table 2).

Ex-cpFSH induced premature cumulus expansion and resumption of meiosis prior to an ovulatory hCG stimulus

The COCs recovered by oocyte retrieval 12 h after the last cpFSH injection (Exps 1 and 3) were classified as comCOCs, expCOCs, or denuded. Only comCOCs or denuded oocytes were recovered by oocyte retrieval in the controls. In contrast, comCOCs, expCOCs, and denuded oocytes were recovered from heifers treated with Ex-cpFSH doses (Table 3, Exps 1 and 3). The proportion of ovulatory-size follicles with expCOCs per heifer was higher ($P < 0.0001$), while the proportion with comCOCs was lower

Table 1 Average fragments per kilobase per million[§] mapped reads values for differential expression of cumulus genes critical for regulation of cumulus function and oocyte maturation in Type 1 compared with Ex-cpFSH-induced Types 2, 3, and 4 ovulatory-size follicles.

Gene symbol	Gene name	Functions	Ovulatory-size follicle types			
			Control	Ex-cpFSH		
			Type 1 (n = 7)	Type 2 (n = 6)	Type 3 (n = 6)	Type 4 (n = 5)
AREG	Amphiregulin	ORM (Procházka et al., 2011; Assidi et al., 2013), CE (Procházka et al., 2011; Assidi et al., 2013)	0	0.1	25	77
CLDN11	Claudin 11	JXN (Gow et al., 1999; Elkouby-Naor and Ben-Yosef, 2010; Zhang et al., 2018)	0.5	100	226	225
FGG	Fibrinogen G Gamma	Cl (Simurda et al., 2020)	0	12	28	98
GPR50	G protein-coupled receptor 50	G (Assidi et al., 2013; Vander Ark et al., 2018), ORM (Chen et al., 2022)	7	2474	2133	1564
IGFBP3	Insulin-like growth factor binding protein 3	G (Yoshimura et al., 1996), ORM (Yoshimura et al., 1996), A (Chun et al., 1994)	3	189	102	243*
IGFBP5	Insulin-like growth factor binding protein 5	G (Onoda et al., 1995), A (Monget et al., 1998; Canty et al., 2006; Hatzirodos et al., 2014; Mazerbourg and Monget, 2018)	15*	479	429	21367
LIF	Leukemia-inhibitory factor	ORM (Dang-Nguyen et al., 2014; Mo et al., 2014), CE (De Matos et al., 2008)	0	2	55	270
MDFI	MyoD family inhibitor	O (Espey, 1978) (Martin et al., 1983)	0	0.8	5	77
MEPE	Matrix extracellular phosphoglycoprotein	ECM (Irving-Rodgers and Rodgers, 2005; Cho et al., 2009; Nagyová et al., 2021)	0	7	1	63
MGAT5	Alpha-1,6-manosyl-gly-coprotein beta-1,6-acetylglucosaminyl-transferase	CE (Lo et al., 2019), ECM (Lo et al., 2019)	56	285	558	1111
NCS1	Neuronal calcium sensor 1	Ca (Rousset et al., 2003; Boeckel and Ehrlich, 2018)	0	0.6	7	60
NGFR	Nerve growth factor receptor	JXN (Zhai et al., 2018), A (Zhou et al., 2016)	0	3	74	97
PLAT	Plasminogen Activator, Tissue	ECM (Rifkin, 1992), CE (Yu, 2019), ORM (Yu, 2019)	39*	673	727	4460
PTX3	Pentraxin 3	CE (Varani et al., 2002), ECM (Baranova et al., 2014; Nagyova et al., 2016; Fan and de Sousa Lope, 2021)	2	122*	4232	5030
RGS2	Regulator of G protein signaling 2	G (Landomiel et al., 2014), Ca (Bernhardt et al., 2015), A (Dong et al., 2017)	0	6	71	102
TGFα	Transforming growth factor alpha	G (Legault et al., 1999), ORM (Brucker et al., 1991; Mito et al., 2013), CE (Kobayashi et al., 1994; Assidi et al., 2013)	0	0.1	9	73
VGF	VGF nerve growth factor inducible	G (Hahm et al., 1999; Aguilar et al., 2013; Choi et al., 2016), Ca (Severini et al., 2007; Bresciani et al., 2019)	0	7	7	193

[§]FPKM values for cumulus DEGs were determined for the Type 1, 2, 3, and 4 ovulatory-size follicles excised from small ovarian reserve Holstein heifers subjected to ovarian stimulation with IS-cpFSH (control) or Ex-cpFSH doses. The number in parentheses under each follicle type indicates the number of individual ovulatory-size follicles and individual animals. Zero = undetectable values. Box Whisker Plots of these results are depicted in Fig. 4. Type 1 ovulatory-size follicles differed ($P < 0.01$, *$P < 0.05$) from Type 2, 3, or 4 follicles for each gene based on DSeq2 analysis. A = apoptosis; Ca = calcium movement; CE = cumulus expansion; Cl = clotting regulation; ECM = extracellular matrix; G = Gonadotrophin action/secretion; JXN = tight junction and cell communication; O = ovulation; ORM = oocyte resumption of meiosis. FPKM, fragments per kilobase per million mapped reads; DEGs, differentially expressed genes; IS-cpFSH, industry-standard commercial FSH-enriched porcine pituitary preparation; Ex-cpFSH, excessive commercial FSH-enriched porcine pituitary preparation.

($P < 0.01$), in the Ex-cpFSH treated heifers compared with controls for Exps 1 and 3 (Table 3).

The impact of the Ex-cpFSH treatment on nuclear maturation prior to the ovulatory hCG stimulus was only examined in Exp 1. Results show that 93% of ovulatory-size follicles in controls and 77% in the Ex-cpFSH treated heifers had comCOCs (Table 3, Exp 1). Of the comCOCs, 77% in controls and 97% in the Ex-cpFSH treated heifers were at the GV stage (Table 4). Although none of the comCOCs had resumed meiosis in controls, a very low proportion (2%) of the ovulatory-size follicles for the heifers treated with the Ex-cpFSH dose had comCOCs that had resumed meiosis (MI, MII, Table 4). However, the proportions of ovulatory-size follicles with comCOCs at MI or MII for the Ex-cpFSH treated heifers did not differ ($P > 0.05$) from controls (Table 4). In contrast to
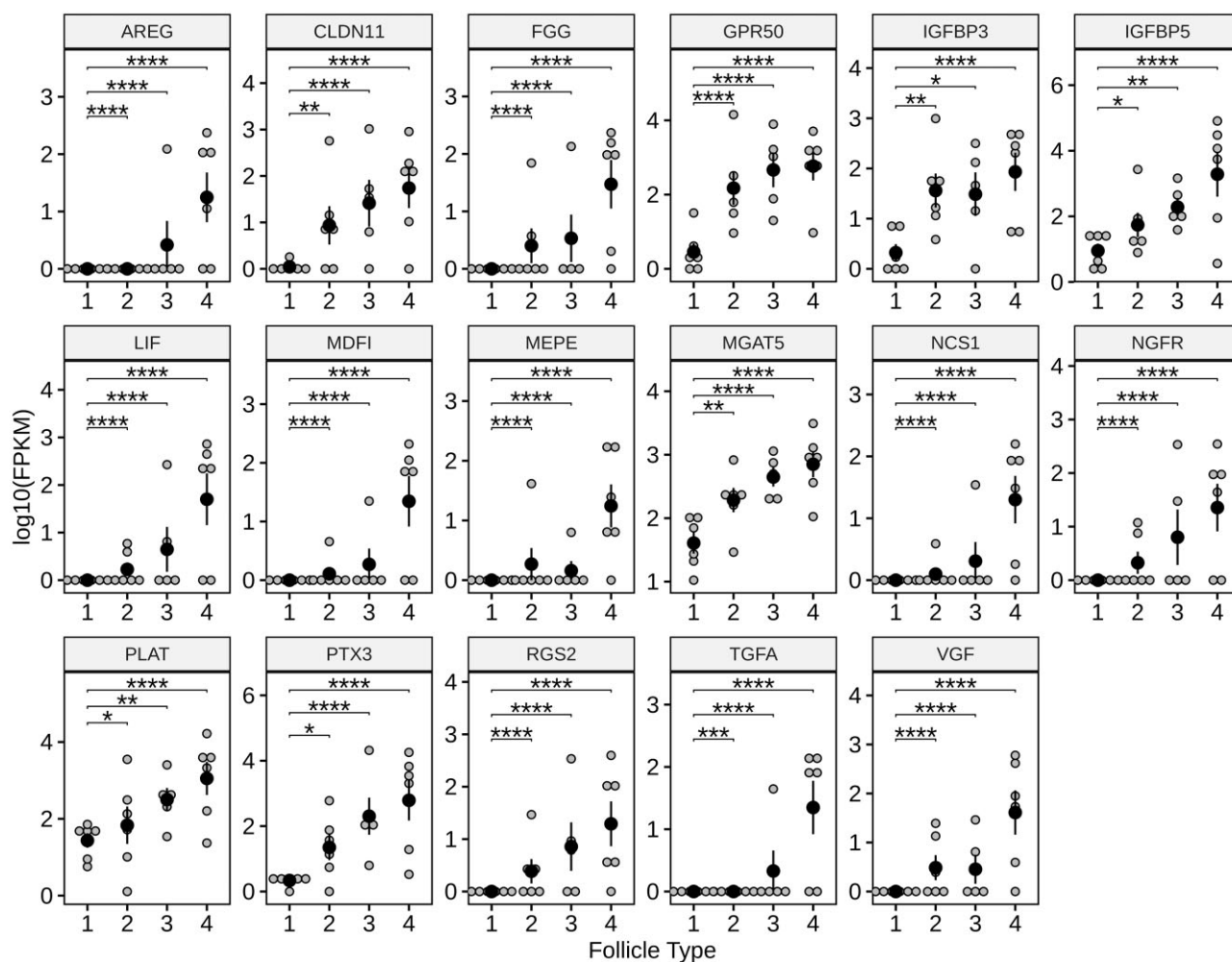
Figure 3. Volcano plots comparing cumulus cell differentially expressed genes for Type 2, 3, and 4 versus 1 ovulatory-size follicles in the small ovarian reserve heifer. Volcano plots of cumulus cell transcriptome data noting locations of the 17 DEGs described in this analysis. Data are from the previously published transcriptome study (Clark *et al.*, 2022b). The panels show data for the comparisons noted above each panel (left to right, Type 2, 3, and 4 versus Type 1). Each panel plots the Log$_2$(foldchange) along the *x* axis, and the $-$Log$_{10}$ (FDR) from the DESeq2 output from our previous study (Clark *et al.*, 2022b). Horizontal dashed lines denote two FDR thresholds: 0.01 and 0.05. Point color key: black = non-DEG; red = upregulated DEGs; blue = downregulated DEGs. The 17 DEGs common to all follicle types are indicated by their gene symbols. DEGs, differentially expressed genes; FDR, false discovery rate.

controls, 22% of the ovulatory-size follicles had expCOCs (Table 3, Exp 1), and 49% of the expCOCs had resumed meiosis (GVBD + MI + MII) in the Ex-cpFSH treated heifers (Table 4). The remainder of the expCOCs in the Ex-cpFSH treated heifers were at the GV stage, had oocytes classified as degenerated or fragmented, or were lost during processing.

Ex-cpFSH blocked cumulus expansion and resumption of meiosis in response to an ovulatory hCG stimulus

In response to the ovulatory hCG stimulus, the proportion of ovulatory-size follicles per heifer with comCOCs was higher ($P < 0.01$) while the proportion with expCOCs was lower ($P < 0.05$) for the heifers treated with Ex-cpFSH doses compared with controls (Table 3, Exp 2). Surprisingly, although prematurely expCOCs (as observed in Exps 1, 3; see Clark *et al.* (2022a,b) for images) could not be distinguished morphologically from expCOCs after the ovulatory hCG stimulus, the proportion of ovulatory-size follicles with expCOCs was nearly identical to the results for the Ex-cpFSH treated heifers in Exps 1, 3 prior to an ovulatory hCG stimulus (Table 3).

We observed that 71% of the expCOCs in controls and 65% of the expCOCs in the Ex-cpFSH treated heifers had resumed meiosis (GVBD + MI + MII) after the ovulatory hCG stimulus (Table 5). The Ex-cpFSH treated heifers had a higher ($P < 0.01$) proportion of ovulatory-size follicles with expCOCs at MI but a lower ($P < 0.001$) proportion at MII, compared with controls. In addition, the Ex-cpFSH treated heifers had a lower ($P < 0.0001$) proportion of ovulatory-size follicles with expCOCs at GV but a higher proportion at MI ($P < 0.01$) and MII ($P < 0.001$) compared with the comCOCs from the Ex-cpFSH treated heifers (Table 5).

After the ovulatory hCG stimulus, we unexpectedly observed that 46% of the ovulatory-size follicles from controls and 72% of the ovulatory-size follicles from heifers treated with the Ex-cpFSH doses had comCOCs (Table 3). Moreover, only 1% of the ovulatory-size follicles with the comCOCs had resumed meiosis in the control compared with ~6% in the Ex-cpFSH treated heifers

(Table 5). Like Exp 1, however, the proportions of ovulatory-size follicles with comCOCs at GVBD, MI, or MII were similar between treatment groups (Table 5).

Ex-cpFSH-induced prematurely expCOCs responded poorly to IVF

The proportion of expCOCs that cleaved and formed blastocysts or hatched blastocysts after IVF was much lower ($P < 0.05$ to $P < 0.0001$) compared with IVF results for IVM-matured comCOCs (Table 6). The very poor cleavage results for expCOCs are unlikely caused by the small number of COCs per IVF group, especially since 12 of 20 (60%) singlets and 38 of 52 (73%) pairs of comCOCs subjected to IVF cleaved by Day 2 of culture.

Ex-cpFSH reduced the capacity of comCOCs and expCOCs recovered prior to an ovulatory hCG stimulus to resume meiosis during IVM

The vast majority (91%) of the ovulatory-size follicle with comCOCs resumed meiosis during IVM (Table 7). Nevertheless, the proportion of ovulatory-size follicles with comCOCs that progressed to MII after IVM was lower ($P < 0.01$) for the Ex-cpFSH treated heifers compared with controls (Table 7). None of the controls had expCOCs as observed in Exp 1. In contrast, 32% of the ovulatory-size follicles recovered 12 h after the last cpFSH injection (prior to the ovulatory hCG stimulus) had expCOCs (Table 3, Exp 3). However, only 38% of the premature expCOCs resumed meiosis and reached MII during IVM, while 55% were classified as degenerated (Table 6). For the Ex-cpFSH treated heifers, the proportion of ovulatory-size follicles with expCOCs that reached MII during IVM was lower ($P < 0.0001$) while the proportion classified as degenerated was higher ($P < 0.05$) compared with comCOCs subjected to IVM (Table 7).

Discussion

The most significant findings in the present study are that Ex-cpFSH doses during the ovarian stimulation of the SORH model:

Figure 4. Expression of cumulus cell genes critical for regulation of cumulus function and oocyte maturation in Type 1 compared with excessive cpFSH-induced Types 2, 3, and 4 ovulatory-size follicles. Small ovarian reserve Holstein heifers in our previous study (Clark *et al.*, 2022b) were subjected to ovarian stimulation with IS-cpFSH (control) or Ex-cpFSH doses and cumulus cells removed from the different types ovulatory-size follicles and subjected to RNAseq and bioinformatic analyses (Table 1 footnote). Types 1, 2, 3, and 4 ovulatory-size follicles are depicted along the x axis. Data points within each panel reflect mean expression values for replicates of each gene based on FPKM (y axis) determined in our previous study (Clark *et al.*, 2022b). Analysis of our previously published data identified 17 shared cumulus DEGs (FDR <0.05 to FDR <0.01) common to all the Type 2, 3, and 4 ovulatory-size follicles. These 17 Ex-cpFSH-induced cumulus cell DEGs all have well-established roles in modulation of FSH action and cumulus cell function including induction of cumulus cell expansion and regulation of oocyte maturation (Table 1). Gene symbols are depicted at the top of each panel (names and functions in Table 1). Within each panel, the large black circles denote mean FPKM values, small gray circles denote each sample, and vertical lines denote SEM. Based on statistical analysis results (using DSeq2 software) from our previous study (Clark *et al.*, 2022b), the horizontal lines at the top of each panel represent comparisons between Type 1 versus 2, 3, or 4 ovulatory-size follicles. Asterisks above each horizontal line indicate if the FDR values for each mean comparison differed significantly (*$P \leq 0.05$, **$P \leq 0.01$, ***$P \leq 0.001$, ****$P \leq 0.0001$). IS-cpFSH, industry-standard commercial FSH-enriched porcine pituitary preparation; Ex-cpFSH, excessive commercial FSH-enriched porcine pituitary preparation; FPKM, fragments per kilobase per million mapped reads; DEG, differentially expressed gene; FDR, false discovery rate.

increase expression of 17 genes in cumulus cells with well-established roles in cumulus expansion, function, and regulation of resumption of meiosis in all ovulatory-size follicles prior to an ovulatory hCG stimulus; induce premature (prior to ovulatory hCG stimulus) expansion of the COC and resumption of meiosis in a moderate proportion of ovulatory-size follicles; impair the capacity of prematurely expCOCs to undergo IVF and resume meiosis during IVM; and reduce responsiveness of comCOCs to an ovulatory hCG stimulus. Taken together, these observations in the SORH biomedical model support the conclusion that excessive FSH doses during ovarian stimulation dysregulate cumulus cell function thereby impairing oocyte quality, contributing to oocyte wastage, and diminishing IVF success and ART outcomes.

The present study extends our previous transcriptome analysis (Clark *et al.*, 2022a,b) by showing that the Ex-cpFSH treatment induces differential expression of a small number of genes (17 of

the 3288) in cumulus cells of all the ovulatory-size follicles independent of their extreme phenotypic differences. Many of these cumulus cell DEGs are regulated directly by FSH (*AREG*, *IGFBP-3*, *IGFBP-5*, *PTX3*, *RGS2*, *TGFα*, *PLAT*, *FGG*) in a variety of species. Moreover, most of these DEGs have well-established critical roles in regulation of gonadotrophin action (*GPR50*, *IGFBP-3*, *IGFBP-5*, *RGS2*) or secretion (*VGF*) and apoptosis (*IGFBP-3*, *IGFBP-5*, *RGS-2*), which could directly dysregulate cumulus cell function. Although *IGFBP-3*, *IGFBP-5*, and *RGS-2* are pro-apoptotic, results of ingenuity pathway analysis in our previous transcriptome study (Clark *et al.*, 2022b) using a robust, high-quality data set did not indicate activation or inhibition of apoptosis. In addition, several of the cumulus cell DEGs identified in the present study are well-established regulators of cumulus expansion (*AREG*, *LIF*, *MGAT5*, *MEPE*, *PTX3*, *TGFα*, *PLAT*) and resumption of meiosis (*AREG*, *IGFBP-3*, *TGFα*, *PLAT*). However, other DEGs impact the extracellular

Table 2 Impact of ovarian stimulation of small ovarian reserve heifers with control or Ex-cpFSH doses on number of ovulatory-size follicles and cumulus–oocyte complex recovery.

	Exp 1		Exp 2		Exp 3	
	Control	Ex-cpFSH	Control	Ex-cpFSH	Control	Ex-cpFSH
Number of ovulatory-size follicles (≥10 mm)	19 ± 5 (6–56)	31 ± 6 (9–59)	21 ± 4 (6–60)	26 ± 4 (9–70)	17 ± 3 (5–46)	19 ± 2 (3–31)
Number of aspirated follicles	16 ± 4 (5–41)	24 ± 4 (8–44)	17 ± 2 (5–32)	20 ± 3 (8–50)	18 ± 3 (13–56)	18 ± 2 (19–45)
Number of COCs recovered by OR	10 ± 3 (2–28)	13 ± 2 (5–26)	12 ± 2 (2–27)	13 ± 2 (2–31)	10 ± 2 (5–41)	11 ± 1 (9–28)
COC recovery rate	58% ± 5% (29–90%)	53% ± 6% (22–85%)	58% ± 3% (33–100%)	63% ± 5% (25–87%)	55% ± 5% (13–100%)	56% ± 5% (10–82%)

The small ovarian reserve Holstein heifers in Exp 1 (n = 10/dose) and 3 (n = 18/dose) were subjected to OR to recover COCs 12 h after the last cpFSH injection while the heifers in Exp 2 (n = 16/dose) were subjected to an ovulatory hCG stimulus 12 h after the last cpFSH injection, and COCs were recovered by OR 24 h after the hCG injection but before ovulation. The number of ovulatory-size follicles was determined at the time of OR. Recovery rate = number of COCs recovered by OR divided by the number of aspirated follicles. Data are expressed as mean ± SEM per heifer with the range of the data collected in parentheses. Based on Type III ANOVA analysis, there were no statistical differences between means. Exp, experiment; IS-cpFSH, industry-standard commercial FSH-enriched porcine pituitary preparation; Ex-cpFSH, excessive commercial FSH-enriched porcine pituitary preparation; OR: oocyte retrieval; COCs, cumulus–oocyte complexes.

Table 3 Impact of ovarian stimulation of small ovarian reserve heifers with control or Ex-cpFSH doses on morphology of cumulus–oocyte complexes.

Morphological classification of COCs	Exp 1		Exp 2		Exp 3	
	Control	Ex-cpFSH	Control	Ex-cpFSH	Control	Ex-cpFSH
comCOC	93% ± 3% (75–100%)	77% ± 4%** (58–100%)	46% ± 9% (0–100%)	72% ± 5%** (27–100%)	91% ± 3% (0–94%)	65% ±5%**** (40–100%)
expCOC	0% ± 0.4% (0–4%)	22% ± 5%**** (0–42%)	45% ± 8% (0–100%)	24% ± 4%* (0–39%)	3% ± 2% (0–29%)	32% ±5%**** (0–82%)
Denuded	3% ± 3% (0–25%)	0.7% ± 1% (0–7%)	7% ± 2% (0–25%)	4% ± 1% (0–17%)	6% ± 3% (0–44%)	3% ± 1% (0–18%)

The small ovarian reserve Holstein heifers in Exp 1 (n = 10/dose) and 3 (n = 18/dose) were subjected to OR to recover COCs 12 h after the last cpFSH injection while the heifers in Exp 2 (n = 16/dose) were subjected to an ovulatory hCG stimulus 12 h after the last cpFSH injection, and COCs were recovered by OR 24 h after the hCG injection but before ovulation. Proportions per column may not total 100% because some COCs or oocytes were unidentifiable or lost during histological processing to assess nuclear maturation. Data are expressed as mean ± SEM for proportions of ovulatory-size follicles per heifer with COCs classified as comCOC, expCOC, or denuded with the range of the data collected in parentheses. * P ≤ 0.05, ** P ≤ 0.01, **** P ≤ 0.0001 denote statistical differences between means within each experiment based on Type III ANOVA analysis. Exp, experiment; IS-cpFSH, industry-standard commercial FSH-enriched porcine pituitary preparation; Ex-cpFSH, excessive commercial FSH-enriched porcine pituitary preparation; OR: oocyte retrieval; COCs, cumulus–oocyte complexes; comCOC, compact cumulus–oocyte complex; expCOC, expanded cumulus–oocyte complex.

Table 4 Impact of ovarian stimulation of small ovarian reserve heifers with control or Ex-cpFSH doses on stage of nuclear maturation for compact cumulus–oocyte complexes or expanded cumulus–oocyte complexes.

	Exp 1		
	Control	Ex-cpFSH	
	comCOC	comCOC	expCOC
Number of oocytes evaluated per heifer	9 ± 3 (1–27)	7 ± 1 (1–14)	3 ± 1 (0–9)
Stage of nuclear maturation			
GV	77% ± 8% (30–100%)	97% ± 3% (75–100%)	19%±10%**** (0–100%)
GVBD	0% ± 0%	0% ± 0%	1% ± 1% (0–11%)
MI	0% ± 0%	1% ± 3% (0–13%)	40% ± 13%** (0–100%)
MII	0% ± 0%	1% ± 1% (0–13%)	8% ± 5% (0–7%)
Degenerated	2% ± 2% (0–14%)	0.8% ± 1% (0–33%)	8% ± 4% (0–33%)

Small ovarian reserve Holstein heifers (n = 10/dose) were subjected to ovarian stimulation with IS-cpFSH (control) or Ex-cpFSH doses then subjected to OR to recover COCs 12 h after the last cpFSH injection. Proportions per column may not total 100% because some COCs or oocytes were unidentifiable or lost during histological processing to assess nuclear maturation. Data are expressed as mean ± SEM for proportion of ovulatory-size follicles with comCOCs or expCOCs at each nuclear maturation stage per heifer with the range of the data collected in parentheses. ** P ≤ 0.01, **** P ≤ 0.0001 denote statistical differences between means within cpFSH dose based on Type III ANOVA analysis. IS-cpFSH, industry-standard commercial FSH-enriched porcine pituitary preparation; Ex-cpFSH, excessive commercial FSH-enriched porcine pituitary preparation; OR: oocyte retrieval; COCs, cumulus–oocyte complexes; comCOC, compact cumulus–oocyte complex; expCOC, expanded cumulus–oocyte complex; GV, germinal vesicle, GVBD, germinal vesicle breakdown; MI, metaphase I; MII, metaphase II.

matrix (*MEPE, MGAT5, PTX3*) and tight junctions and cell communication (*CLDN11, NGFR*), including calcium movement (*NCS1, RGS2, VGF*) in non-cumulus cell types that could also have an undiscovered yet critical role in cumulus function and capacity to regulate resumption of meiosis. Two DEGs serve other roles in cumulus cells (*FGG, MDFI*). FGG has a role in regulation of blood

Table 5 Impact of an ovulatory hCG stimulus following ovarian stimulation of small ovarian reserve heifers with control or Ex-cpFSH doses on stage of nuclear maturation for compact cumulus–oocyte complexes or expanded cumulus–oocyte complexes.

	Exp 2			
	Control		Ex-cpFSH	
	comCOC	expCOC	comCOC	expCOC
Number of oocytes evaluated per heifer	2 ± 0.5 (0–6)	4 ± 1 (0–14)	4 ± 0.8 (1–13)	3 ± 0.7 (0–9)
Stage of nuclear maturation				
GV	68% ± 12% (0–100%)	4% ± 3%[***] (0–40%)	86% ± 3%[++] (50–100%)	11% ± 5%[****] (0–50%)
GVBD	1% ± 1% (0–17%)	2% ± 2% (0–25%)	4% ± 3% (0–50%)	0.7% ± 1% (0–11%)
MI	0% ± 0%	12% ± 6%[*] (0–75%)	1% ± 1% (0–17%)	30% ± 10%[**] (0–100%)
MII	0% ± 0%	57% ± 12%[****] (0–100%)	0.7% ± 1% (0–11%)	34% ± 8%[++++***] (0–100%)
Degenerated	0% ± 0%	0% ± 0%	7% ± 6% (0–11%)	7% ± 3% (0–50%)

Small ovarian reserve Holstein heifers were subjected to ovarian stimulation with IS-cpFSH (control, n = 15) or Ex-cpFSH (n = 16) doses and then subjected to an ovulatory hCG stimulus 12 h after the last cpFSH injection, and COCs were recovered by OR 24 h after the hCG injection but before ovulation. Proportions per column may not total 100% because some COCs or oocytes were unidentifiable or lost during histological processing to assess nuclear maturation. Proportions per column may not total 100% because some COCs or oocytes were unidentifiable or lost during histological processing to assess nuclear maturation. Data are expressed as means ± SEM for proportion of ovulatory-size follicles with COCs at each nuclear classification per heifer with the range of the data collected in parentheses. * $P \leq 0.05$, ** $P \leq 0.01$, *** $P \leq 0.001$. **** $P \leq 0.0001$ denote statistical differences between means but within COC classification across cpFSH doses based on Type III ANOVA analysis. IS-cpFSH, industry-standard commercial FSH-enriched porcine pituitary preparation; Ex-cpFSH, excessive commercial FSH-enriched porcine pituitary preparation; OR, oocyte retrieval; COCs, cumulus–oocyte complexes; comCOC, compact cumulus–oocyte complex; expCOC, expanded cumulus–oocyte complex; GV, germinal vesicle, GVBD, germinal vesicle breakdown; MI, metaphase I; MII, metaphase II.

Table 6 IVF results for bovine oocytes with prematurely expanded or compact layers of cumulus cells.

	Exp 3			
COC morphology	N	Cleaved	Blastocyst	Hatched Blastocyst
comCOC	182	124 (68%)	51 (28%)	22 (12%)
expCOC	37	2 (5.4%)[****]	0 (0%)[***]	0 (0%)[*]

The comCOC were recovered from follicles of ovaries obtained at a local abattoir and subjected to IVM and IVF. Prematurely expCOC were obtained from Ex-cpFSH treated heifers (n = 8) 12 h after the last cpFSH injection but prior to an ovulatory hCG stimulus and subjected to IVF (using sperm from the same bull) without IVM. Data are represented as the number of fertilized oocytes from comCOC or expCOC subjected to IVF that cleaved, formed blastocysts, or hatched blastocysts divided by total number of comCOC or expCOC subjected to IVF with the ratio in parentheses. * $P \leq 0.05$, *** $P \leq 0.001$, **** $P \leq 0.0001$ denote significant difference between ratios when comCOC were compared with expCOC based on Type III ANOVA analysis. comCOC, compact cumulus–oocyte complex; expCOC, expanded cumulus–oocyte complex; Ex-cpFSH, excessive commercial FSH-enriched porcine pituitary preparation; N, number of comCOC or expCOC.

clotting (Simurda *et al.*, 2020) and *MDFI* inhibits myogenesis (Berkes and Tapscott, 2005) and may have a role in ovulation (Espey, 1978; Martin *et al.*, 1983). Thus, dysregulation of *FGG* and *MDFI* could contribute to the reduced ovulation rate observed for the heifers subjected to Ex-cpFSH during ovarian stimulation in our previous study (Karl *et al.*, 2021).

Taken together, the discovery of DEGs overexpressed in cumulus cells in response to Ex-cpFSH in all of the ovulatory-size follicles of Ex-cpFSH dosed animals provides new insight into potential mechanisms whereby excessive FSH action prior to an ovulatory hCG stimulus induces premature cumulus expansion, as observed in our previous (Clark *et al.*, 2022a,b) and present studies, and premature resumption of meiosis.

The 17 cumulus cell DEGs reported here for Ex-cpFSH treated heifers are induced prior to an ovulatory hCG stimulus and many of these genes are known to be involved in cumulus expansion. However, even though these DEGs are in COCs of all ovulatory-size follicles, we observed here and in our previous studies (Clark *et al.*, 2022a,b) that premature cumulus expansion did not occur in all ovulatory-size follicles. This disconnect very likely represents a potential lag between the Ex-cpFSH induced alterations in gene expression with initiation of the morphological changes causing cumulus expansion (e.g. extracellular matrix). In addition, differential responsiveness of ovulatory-size follicles to cpFSH, which may explain the high within animal variability observed in gene expression (Box Whisker Plots, Fig. 4), could also contribute to the disconnect between expression of genes involved in cumulus expansion and cumulus expansion.

In the Ex-cpFSH treated heifers, a high proportion (75%) of ovulatory-size follicle had expCOCs in our previous study (Clark *et al.*, 2022a,b) while only a moderate proportion (22% for Exp 1, 32% for Exp 3) of ovulatory-size follicles had expCOCs in the present study. We cannot rule out the possibility that animal variation or differences in cpFSH potency explain the differences in proportion of ovulatory-size follicles with expCOCs between our present and previous (Clark *et al.*, 2022a,b) studies. However, it is highly likely that expCOCs, often described as very sticky in a variety of species (Moulavi and Hosseini, 2018; Richards, 2018), are more fragile and difficult to remove from ovulatory-size follicles during oocyte retrieval than comCOCs. For example, oocyte retrieval damages COCs if the aspiration pressure is not optimal (Ward *et al.*, 2000; Rose, 2014; Renzini *et al.*, 2020), which could explain why denuded oocytes were observed after oocyte retrieval in the present study. Consistent with this possible explanation, denuded oocytes were not observed when COCs were removed from excised ovulatory-size follicles using gentle pressure on a syringe and needle, as in our previous study (Clark *et al.*, 2022a,b).

We recognize a larger number of the Ex-cpFSH induced prematurely expanded COCs (expCOCs) from additional cattle will be necessary to confirm the inferior IVF results compared with not only controls in the present study but also with typical IVF results following IVM or artificial insemination of cattle reported by others (Lonergan and Fair, 2016). Nevertheless, our findings indicate that the prematurely expanded COCs observed here are defective and have poor-quality oocytes. The precise reason for diminished oocyte competence is unknown but very likely arises owing to dysregulated progression through meiosis (Table 4). However, we also observed in the present study that nearly 38% of the expCOCs recovered by oocyte retrieval before an ovulatory hCG stimulus reached the MII stage during IVM. This finding implies that IVM of the prematurely expanded COCs could have improved the poor IVF results observed in the present study

Table 7 Impact of ovarian stimulation of small ovarian reserve heifers with control or Ex-cpFSH doses on stage of nuclear maturation of compact cumulus–oocyte complexes or expanded cumulus–oocyte complexes after IVM.

	Exp 3		
	Control	Ex-cpFSH	
	comCOC	comCOC	expCOC
Number of oocytes evaluated per heifer	9 ± 2 (2–33)	7 ± 1 (2–20)	4 ± 0.8 (0–11)
Stage of nuclear maturation after IVM			
GV	8% ± 3% (0–43%)	9% ± 2% (0–25%)	8% ± 6% (0–50%)
GVBD	6% ± 2% (0–25%)	5% ± 2% (0–25%)	0% ± 0%
MI	3% ± 2% (0–33%)	6% ± 2% (0–25%)	0% ± 0%
MII	82% ± 4% (50–100%)	70%±6%[++] (17–100%)	38%±16%[****] (0–100%)
Degenerated	1% ± 1% (0–9%)	10% ± 4% (0–50%)	55% ± 14%[*] (0–100%)

COCs were recovered from small ovarian reserve Holstein heifers subjected to ovarian stimulation with IS-cpFSH (control, n = 17 heifers) or Ex-cpFSH (n = 14) doses and IVM for 22 h. Proportions per column may not total 100% because some COCs or oocytes were unidentifiable or lost during histological processing to assess nuclear maturation. Data are expressed as mean ± SEM for proportion of ovulatory-size follicles with comCOCs or expCOCs at each nuclear maturation stage per heifer with the range of the data collected in parentheses. [*] $P \leq 0.05$, [****] $P \leq 0.0001$ denote statistical differences between means within cpFSH dose whereas pluses. ([++] $P \leq 0.01$) denote statistical difference between means across dose but within COC classification across cpFSH doses based on Type III ANOVA analysis. COCs, cumulus–oocyte complexes; IS-cpFSH, industry-standard commercial FSH-enriched porcine pituitary preparation; Ex-cpFSH, excessive commercial FSH-enriched porcine pituitary preparation; comCOC, compact cumulus–oocyte complex; expCOC, expanded cumulus–oocyte complex; GV, germinal vesicle, GVBD, germinal vesicle breakdown; MI, metaphase I; MII, metaphase II.

(Table 6), although this was not examined. Nevertheless, we observed that the moderate proportion of ovulatory-size follicles with prematurely expanded COCs developing to MII during IVM was highly variable amongst heifers, while a higher proportion had degenerated during IVM (Table 5). Thus, we expect that IVM of prematurely expanded COCs would only marginally improve IVF success for a limited number of heifers.

We established that Ex-cpFSH doses during ovarian stimulation of the SORH model reduced estradiol production (Karl *et al.*, 2021; Clark *et al.*, 2022a,b) and decreased the hCG-induced ovulation rate (Karl *et al.*, 2021). These findings indicated that the Ex-cpFSH doses during ovarian stimulation impair responsiveness of ovulatory-size follicles to an ovulatory hCG stimulus. If so, this could explain why both estradiol production and ovulation rate were reduced in our previous studies (Karl *et al.*, 2021). Results here further confirm the likelihood that Ex-cpFSH doses diminish the responsiveness of ovulatory-size follicles to an ovulatory hCG stimulus based on three comparisons. First, after the ovulatory hCG stimulus, the proportion of ovulatory-size follicles per heifer with comCOCs (Table 3, Exp 2) and proportion of comCOCs that remained at the GV stage (Table 5) were both higher in the Ex-cpFSH treated heifers compared with controls. Second, the proportions of ovulatory-size follicles per heifer treated with Ex-cpFSH doses that had comCOCs and expCOCs before (Table 3, Exp 1) and after (Table 3, Exp 2) the ovulatory hCG stimulus were nearly identical. Third, a higher proportion of the expCOCs remained at GV while a lower proportion reached MII in the Exp-cpFSH treated heifers compared with controls (Table 5) implying that the Exp-cpFSH doses impeded resumption and progression of nuclear maturation to MII. These combined findings, coupled with our previous results (Karl *et al.*, 2021; Clark *et al.*, 2022a,b), provide compelling evidence that the Ex-cpFSH treatment during ovarian stimulation (prior to the ovulatory hCG stimulus) blocks responsiveness of the ovulatory-size follicles to hCG thereby reducing availability of high-quality hCG-matured COCs for ART.

Previous studies in sheep show that typical ovarian stimulation regimens do not enhance responsiveness of all ovulatory-size follicles to FSH or LH (McNatty *et al.*, 2010). This observation may explain why, although lower than the Ex-cpFSH treated heifers, a relatively high proportion (46%) of ovulatory-size follicles per heifer in controls had comCOCs after the ovulatory hCG stimulus. While the precise reason is unclear, the results imply that ovarian stimulation, even with the industry-standard cpFSH doses (control), also hinders responsiveness to an ovulatory hCG stimulus. In support of this possibility, results of our previous study (Karl *et al.*, 2021) show that ~20% of the ovulatory-size follicles per heifer developing in response to the control doses do not ovulate in response to an ovulatory hCG stimulus.

In summary, the results identified key Ex-cpFSH-induced DEGs in cumulus cells that may dysregulate cumulus function, enhance premature cumulus expansion, and impair oocyte quality in ovulatory-size follicles developing prior to an ovulatory hCG stimulus. In addition, the excessive FSH also induced inhibition of cumulus expansion and oocyte maturation post-hCG, and a reduced capacity of oocytes with prematurely expanded cumulus cells to undergo IVF or nuclear maturation during IVM. Although cumulus expansion is the hallmark for oocyte maturation in response to a preovulatory LH surge (Eppig, 1982; Ng *et al.*, 1999; Nevoral *et al.*, 2015; Robker *et al.*, 2018), our observations emphasize the risks of recovery of predominantly dysregulated COCs. Such compromised COCs are likely morphologically indistinguishable from high-quality hCG-matured COCs, which could diminish IVF success rates when excessive FSH doses are used during ovarian stimulation.

Data availability

Data generated in the article is available upon reasonable request to the corresponding author.

Acknowledgements

Beef Co., Hudsonville, MI, for the donation of ovaries for our studies.

Authors' roles

K.K., K.L., and J.I. designed the studies; K.K., Z.C., M.R., and J.C. performed experiments; K.K., Z.C., and P.S. analyzed the data; R.T. provided statistical advice; K.K., K.L., and J.I. interpreted the results; and K.K. and J.I. wrote the article. All authors edited the article, approved the final version of the manuscript, and are accountable for all aspects of the work.

Funding

Conflict of interest

The authors declare no conflict of interest.

References

Abdalla H, Thum MY. An elevated basal FSH reflects a quantitative rather than qualitative decline of the ovarian reserve. *Hum Reprod* 2004;**19**:893–898.

Aguilar E, Pineda R, Gaytán F, Sánchez-Garrido MA, Romero M, Romero-Ruiz A, Ruiz-Pino F, Tena-Sempere M, Pinilla L. Characterization of the reproductive effects of the Vgf-derived peptide TLQP-21 in female rats: in vivo and in vitro studies. *Neuroendocrinology* 2013;**98**:38–50.

Assidi M, Richard FJ, Sirard MA. FSH in vitro versus LH in vivo: similar genomic effects on the cumulus. *J Ovarian Res* 2013;**6**:68.

Baker VL, Brown MB, Luke B, Smith GW, Ireland JJ. Gonadotropin dose is negatively correlated with live birth rate: analysis of more than 650,000 assisted reproductive technology cycles. *Fertil Steril* 2015;**104**:1145–1152.

Baranova NS, Inforzato A, Briggs DC, Tilakaratna V, Enghild JJ, Thakar D, Milner CM, Day AJ, Richter RP. Incorporation of pentraxin 3 into hyaluronan matrices is tightly regulated and promotes matrix cross-linking. *J Biol Chem* 2014;**289**:30481–30498.

Berkes CA, Tapscott SJ. Myod and the transcriptional control of myogenesis. *Semin Cell Dev Biol* 2005;**16**:585–595.

Bernhardt ML, Lowther KM, Padilla-Banks E, McDonough CE, Lee KN, Evsikov AV, Uliasz TF, Chidiac P, Williams CJ, Mehlmann LM. Regulator of g-protein signaling 2 (RGS2) suppresses premature calcium release in mouse eggs. *Development* 2015;**142**:2633–2640.

Boeckel GR, Ehrlich BE. NCS-1 is a regulator of calcium signaling in health and disease. *Biochim Biophys Acta Mol Cell Res* 2018;**1865**:1660–1667.

Bresciani E, Possenti R, Coco S, Rizzi L, Meanti R, Molteni L, Locatelli V, Torsello A. TLQP-21, a VGF-derived peptide endowed of endocrine and extraendocrine properties: focus on in vitro calcium signaling. *Int J Mol Sci* 2019;**21**:130.

Brucker C, Alexander NJ, Hodgen GD, Sandow BA. Transforming growth factor-alpha augments meiotic maturation of cumulus cell-enclosed mouse oocytes. *Mol Reprod Dev* 1991;**28**:94–98.

Burns DS, Jimenez-Krassel F, Ireland JLH, Knight PG, Ireland JJ. Numbers of antral follicles during follicular waves in cattle: evidence for high variation among animals, very high repeatability in individuals, and an inverse association with serum follicle-stimulating hormone concentrations. *Biol Reprod* 2005;**73**:54–62.

Canty MJ, Boland MP, Evans ACO, Crowe MA. Alterations in follicular IGFBP mRNA expression and follicular fluid IGFBP concentrations during the first follicle wave in beef heifers. *Anim Reprod Sci* 2006;**93**:199–217.

Centers for Disease Control and Prevention ASfRM, Society for Assisted Reproductive Technology. *Assisted Reproductive Technology National Summary Report*. Atlanta, GA: US Dept of Health and Human Services, 2013.

Chen Y, Zeng R, Kou J, Xiong X, Yao Y, Fu W, Yin S, Lan D. GPR50 participates in and promotes yak oocyte maturation: a new potential oocyte regulatory molecule. *Theriogenology* 2022;**181**:34–41.

Cho YD, Yoon WJ, Woo KM, Baek JH, Lee G, Cho JY, Ryoo HM. Molecular regulation of matrix extracellular phosphoglycoprotein expression by bone morphogenetic protein-2. *J Biol Chem* 2009;**284**:25230–25240.

Choi SG, Wang Q, Jia J, Chikina M, Pincas H, Dolios G, Sasaki K, Wang R, Minamino N, Salton SRJ *et al.* Characterization of gonadotrope secretoproteome identifies neurosecretory protein VGF-derived peptide suppression of follicle-stimulating hormone gene expression. *J Biol Chem* 2016;**291**:21322–21334.

Chun SY, Billig H, Tilly JL, Furuta I, Tsafriri A, Hsueh AJ. Gonadotropin suppression of apoptosis in cultured preovulatory follicles: mediatory role of endogenous insulin-like growth factor I. *Endocrinology* 1994;**135**:1845–1853.

Clark ZL, Karl KR, Ruebel ML, Latham KE, Ireland JJ. Excessive follicle-stimulating hormone during ovarian stimulation of cattle may induce premature luteinization of most ovulatory-size follicles. *Biol Reprod* 2022a;**106**:968–978.

Clark ZL, Ruebel ML, Schall PZ, Karl KR, Ireland JJ, Latham KE. Follicular hyperstimulation dysgenesis: new explanation for adverse effects of excessive FSH in ovarian stimulation. *Endocrinology* 2022b;**163**:1–19.

Clark ZL, Thakur M, Leach RE, Ireland JJ. FSH dose is negatively correlated with number of oocytes retrieved: analysis of a data set with ~650,000 art cycles that previously identified an inverse relationship between FSH dose and live birth rate. *J Assist Reprod Genet* 2021;**38**:1787–1797.

Dang-Nguyen TQ, Haraguchi S, Kikuchi K, Somfai T, Bodó S, Nagai T. Leukemia inhibitory factor promotes porcine oocyte maturation and is accompanied by activation of signal transducer and activator of transcription 3. *Mol Reprod Dev* 2014;**81**:230–239.

De Matos DG, Miller K, Scott R, Tran CA, Kagan D, Nataraja SG, Clark A, Palmer S. Leukemia inhibitory factor induces cumulus expansion in immature human and mouse oocytes and improves mouse two-cell rate and delivery rates when it is present during mouse in vitro oocyte maturation. *Fertil Steril* 2008;**90**:2367–2375.

Donaldson LE. Dose of FSH-P as a source of variation in embryo production from superovulated cows. *Theriogenology* 1984;**22**:205–212.

Donaldson LE, Perry B. Embryo production by repeated superovulation of commercial donor cows. *Theriogenology* 1983;**20**:163–168.

Dong H, Zhang Y, Wang J, Kim DS, Wu H, Sjögren B, Gao W, Luttrell L, Wang H. Regulator of G protein signaling 2 is a key regulator of pancreatic β-cell mass and function. *Cell Death Dis* 2017;**8**:e2821.

Edwards RG, Lobo R, Bouchard P. Time to revolutionize ovarian stimulation. *Hum Reprod* 1996;**11**:917–919.

Elkouby-Naor L, Ben-Yosef T. *Functions of Claudin Tight Junction Proteins and Their Complex Interactions in Various Physiological systems. Int Rev Cell Mol Biol* 2010;**279**:1–32.

Eppig JJ. The relationship between cumulus cell-oocyte coupling, oocyte meiotic maturation, and cumulus expansion. *Dev Biol* 1982;**89**:268–272.

Espey LL. Ovarian contractility and its relationship to ovulation: a review. *Biol Reprod* 1978;**19**:540–551.

Fan X, de Sousa Lopes SM. Molecular makeup of the human adult ovary. *Curr Opin Endocrin Metab* 2021;**18**:187–193.

Gow A, Southwood CM, Li JS, Pariali M, Riordan GP, Brodie SE, Danias J, Bronstein JM, Kachar B, Lazzarini RA. CNS myelin and sertoli cell tight junction strands are absent in Osp/claudin-11 null mice. *Cell* 1999;**99**:649–659.

Greve T, Lehn-Jensen H, Rasbech NO. Morphological evaluation of bovine embryos recovered non-surgically from superovulated dairy cows on days 6 1/2 to 7 1/2: a field study. *Ann Biol Anim Biochem Biophys* 1979;**19**:1599–1611.

Hahm S, Mizuno TM, Wu TJ, Wisor JP, Priest CA, Kozak CA, Boozer CN, Peng B, McEvoy RC, Good P *et al.* Targeted deletion of the Vgf gene indicates that the encoded secretory peptide precursor plays a novel role in the regulation of energy balance. *Neuron* 1999;**23**:537–548.

Hatzirodos N, Hummitzsch K, Irving-Rodgers HF, Harland ML, Morris SE, Rodgers RJ. Transcriptome profiling of granulosa cells from bovine ovarian follicles during atresia. *BMC Genom* 2014;**15**:1–26.

Hazekamp J, Bergh C, Wennerholm UB, Hovatta O, Karlström PO, Selbing A. Avoiding multiple pregnancies in art: consideration of new strategies. *Hum Reprod* 2000;**15**:1217–1219.

Inge GB, Brinsden PR, Elder KT. Oocyte number per live birth in IVF: Were Steptoe and Edwards less wasteful? *Hum Reprod* 2005;**20**:588–592.

Ireland J, Ward F, Jimenez-Krassel F, Ireland JLH, Smith GW, Lonergan P, Evans ACO. Follicle numbers are highly repeatable within individual animals but are inversely correlated with FSH concentrations and the proportion of good-quality embryos after ovarian stimulation in cattle. *Hum Reprod* 2007;**22**:1687–1695.

Ireland JJ, Roche JF. Development of antral follicles in cattle after prostaglandin-induced luteolysis: changes in serum hormones, steroids in follicular fluid, and gonadotropin receptors. *Endocrinology* 1982;**111**:2077–2086.

Ireland JJ, Roche JF. Growth and differentiation of large antral follicles after spontaneous luteolysis in heifers: changes in concentration of hormones in follicular fluid and specific binding of gonadotropins to follicles. *J Anim Sci* 1983;**57**:157–167.

Ireland JJ, Smith GW, Scheetz D, Jimenez-Krassel F, Folger JK, Ireland JLH, Mossa F, Lonergan P, Evans ACO. Does size matter in females? An overview of the impact of the high variation in the ovarian reserve on ovarian function and fertility, utility of anti-Müllerian hormone as a diagnostic marker for fertility and causes of variation in the ovarian reserve in cattle. *Reprod Fertil Dev* 2011;**23**:1–14.

Ireland JJ, Zielak-Steciwko AE, Jimenez-Krassel F, Folger J, Bettegowda A, Scheetz D, Walsh S, Mossa F, Knight PG, Smith GW *et al.* Variation in the ovarian reserve is linked to alterations in intrafollicular estradiol production and ovarian biomarkers of follicular differentiation and oocyte quality in cattle. *Biol Reprod* 2009;**80**:954–964.

Ireland JLH, Scheetz D, Jimenez-Krassel F, Themmen APN, Ward F, Lonergan P, Smith GW, Perez GI, Evans ACO, Ireland JJ. Antral follicle count reliably predicts number of morphologically healthy oocytes and follicles in ovaries of young adult cattle. *Biol Reprod* 2008;**79**:1219–1225.

Irving-Rodgers HF, Rodgers RJ. Extracellular matrix in ovarian follicular development and disease. *Cell Tissue Res* 2005;**322**:89–98.

Jimenez-Krassel F, Folger JK, Ireland JLH, Smith GW, Hou X, Davis JS, Lonergan P, Evans ACO, Ireland JJ. Evidence that high variation in ovarian reserves of healthy young adults has a negative impact on the corpus luteum and endometrium during estrous cycles in cattle. *Biol Reprod* 2009;**80**:1272–1281.

Karabon P. Rare events or non-convergence with a binary outcome? The power of firth regression in proc logistic. *SAS Gf* 2020. https://www.sas.com/content/dam/SAS/support/en/sas-global-forum proceedings/2020/4654-2020.pdf.

Karl KR, Jimenez-Krassel F, Gibbings E, Ireland JLH, Clark ZL, Tempelman RJ, Latham KE, Ireland JJ. Negative impact of high doses of follicle-stimulating hormone during superovulation on the ovulatory follicle function in small ovarian reserve dairy heifers. *Biol Reprod* 2021;**104**:695–705.

Klinkert ER, Broekmans FJ, Looman CW, Habbema JD, Te Velde ER. Expected poor responders on the basis of an antral follicle count do not benefit from a higher starting dose of gonadotrophins in IVF treatment: a randomized controlled trial. *Hum Reprod* 2005;**20**:611–615.

Kobayashi K, Yamashita S, Hoshi H. Influence of epidermal growth factor and transforming growth factor-α on in vitro maturation of cumulus cell-enclosed bovine oocytes in a defined medium. *J Reprod Fertil* 1994;**100**:439–446.

Kovalevsky G, Patrizio P. High rates of embryo wastage with use of assisted reproductive technology: a look at the trends between 1995 and 2001 in the united states. *Fertil Steril* 2005;**84**:325–330.

Landomiel F, Gallay N, Jégot G, Tranchant T, Durand G, Bourquard T, Crépieux P, Poupon A, Reiter E. Biased signalling in follicle stimulating hormone action. *Mol Cell Endocrinol* 2014;**382**:452–459.

Legault S, Bailey JL, Fortier MA, Rouillier P, Guilbault LA. Intracellular regulation of estradiol and progesterone production by cultured bovine granulosa cells. *Mol Reprod Dev* 1999;**54**:371–378.

Lo BKM, Archibong-Omon A, Ploutarchou P, Day AJ, Milner CM, Williams SA. Oocyte-specific ablation of n- and o-glycans alters cumulus cell signalling and extracellular matrix composition. *Reprod Fertil Dev* 2019;**31**:529–537.

Lodde V, Modina S, Galbusera C, Franciosi F, Luciano AM. Large-scale chromatin remodeling in germinal vesicle bovine oocytes: interplay with gap junction functionality and developmental competence. *Mol Reprod Dev* 2007;**74**:740–749.

Lonergan P, Fair T. Maturation of oocytes in vitro. *Annu Rev Anim Biosci* 2016;**4**:255–268.

Love MI, Huber W, Anders S. Moderated estimation of fold change and dispersion for RNA-seq data with DESeq2. *Genome Biol* 2014;**15**:550.

Martin GG, van Steenwyk G, Miller-Walker C. The fate of thecal smooth muscle cells in postovulatory hamster follicles. *Anat Rec* 1983;**207**:267–277.

Mazerbourg S, Monget P. Insulin-like growth factor binding proteins and IGFBP proteases: a dynamic system regulating the ovarian folliculogenesis. *Front Endocrinol* 2018;**9**:1–10.

McGowan MR, Braithwaite M, Jochle W, Maplecoft RJ. Superovulation of beef heifers with Pergonal (HMG): a dose response trial. *Theriogenology* 1985;**24**:173–184.

McNatty KP, Heath DA, Hudson NL, Reader KL, Quirke L, Lun S, Juengel JL. The conflict between hierarchical ovarian follicular development and superovulation treatment. *Reproduction* 2010;**140**:287–294.

Mito T, Yoshioka K, Noguchi M, Yamashita S, Hoshi H. Recombinant human follicle-stimulating hormone and transforming growth factor-alpha enhance in vitro maturation of porcine oocytes. *Mol Reprod Dev* 2013;**80**:549–560.

Mo X, Wu G, Yuan D, Jia B, Liu C, Zhu S, Hou Y. Leukemia inhibitory factor enhances bovine oocyte maturation and early embryo development. *Mol Reprod Dev* 2014;**81**:608–618.

Monget P, Pisselet C, Monniaux D. Expression of insulin-like growth factor binding protein-5 by ovine granulosa cells is regulated by cell density and programmed cell death in vitro. *J Cell Physiol* 1998;**177**:13–25.

Mossa F, Jimenez-Krassel F, Walsh S, Berry DP, Butler ST, Folger J, Smith GW, Ireland JLH, Lonergan P, Ireland JJ *et al.* Inherent capacity of the pituitary gland to produce gonadotropins is not influenced by the number of ovarian follicles 3 mm in diameter in cattle. *Reprod Fertil Dev* 2010;**22**:550–557.

Moulavi F, Hosseini SM. Diverse patterns of cumulus cell expansion during in vitro maturation reveal heterogeneous cellular and molecular features of oocyte competence in dromedary camel. *Theriogenology* 2018;**119**:259–267.

Nagyova E, Kalous J, Nemcova L. Increased expression of pentraxin 3 after in vivo and in vitro stimulation with gonadotropins in porcine oocyte-cumulus complexes and granulosa cells. *Domest Anim Endocrinol* 2016;**56**:29–35.

Nagyová E, Němcová L, Camaioni A. Cumulus Extracellular Matrix Is an Important Part of Oocyte Microenvironment in Ovarian Follicles: Its Remodeling and Proteolytic Degradation. *IJMS* 2021;**23**:54.

Nevoral J, Orsák M, Klein P, Petr J, Dvořáková M, Weingartová I, Vyskočilová A, Zámostná K, Krejčová T, Jílek F. Cumulus cell expansion, its role in oocyte biology and perspectives of measurement: a review. *Sci Agric Bohem* 2015;**45**:212–225.

Ng ST, Chang TH, Wu TC. Prediction of the rates of fertilization, cleavage, and pregnancy success by cumulus-coronal morphology in an in vitro fertilization program. *Fertil Steril* 1999;**72**:412–417.

Onoda N, Li D, Mickey G, Erickson G, Shimasaki S. Gonadotropin-releasing hormone overcomes follicle-stimulating hormone's inhibition of insulin-like growth factor-5 synthesis and promotion of its degradation in rat granulosa cells. *Mol Cell Endocrinol* 1995;**110**:17–25.

Pal L, Jindal S, Witt BR, Santoro N. Less is more: increased gonadotropin use for ovarian stimulation adversely influences clinical pregnancy and live birth after in vitro fertilization. *Fertil Steril* 2008;**89**:1694–1701.

Patel OV, Bettegowda A, Ireland JJ, Coussens PM, Lonergan P, Smith GW. Functional genomics studies of oocyte competence: evidence that reduced transcript abundance for follistatin is associated with poor developmental competence of bovine oocytes. *Reproduction* 2007;**133**:95–106.

Pawlyshyn V, Lindsell CE, Braithwaite M, Mapletoft RJ. Superovulation of beef cows with FSH-P: a dose-response trail. *Theriogenology* 1986;**25**:179.

Prentice-Biensch J, Singh J, Alfoteisy B, Anzar M. A simple and high-throughput method to assess maturation status of bovine oocytes: comparison of anti-lamin A/C-DAPI with an aceto-orcein staining technique. *Theriogenology* 2012;**78**:1633–1638.

Procházka R, Petlach M, Nagyová E, Nemcová L. Effect of epidermal growth factor-like peptides on pig cumulus cell expansion, oocyte maturation, and acquisition of developmental competence in vitro: comparison with gonadotropins. *Reproduction* 2011;**141**:425–435.

Renzini MM, Brigante C, Zanirato MD, Canto MB, Brambillasca F, Fadini R. Oocyte retrieval in IVM. In: Malvasi A, Baldini D (eds), *Pick up and Oocyte Management*. Cham: Springer International Publishing, 2020, p. 195–207.

Richards JS. Ovulation. In: Skinner MK (ed.), *Encyclopedia of Reproduction*, 2nd edn. Oxford: Academic Press, 2018, p. 92–98.

Rifkin DB. Plasminogen activator expression and matrix degradation. *Matrix Suppl* 1992;**1**:20–22.

Robker RL, Hennebold JD, Russell DL. Coordination of ovulation and oocyte maturation: a good egg at the right time. *Endocrinology* 2018;**159**:3209–3218.

Rose BI. Approaches to oocyte retrieval for advanced reproductive technology cycles planning to utilize in vitro maturation: a review of the many choices to be made. *J Assist Reprod Genet* 2014;**31**:1409–1419.

Rousset M, Cens T, Gavarini S, Jeromin A, Charnet P. Down-regulation of voltage-gated Ca^{2+} channels by neuronal calcium sensor-1 is β; subunit-specific. *J Biol Chem* 2003;**278**:7019–7026.

SAS Inc. SAS/Stat® 13.1 User's Guide Introduction to Power and Sample Size Analysis. SAS Institute Inc., 2013.

SAS Inc. SAS/Stat®14.1 User's Guide the Logistic Procedure. SAS Institute Inc., 2015.

SAS Inc. SAS/Share® 9.4: User's Guide, 2nd edn. Cary, NC: SAS Institute Inc., 2019.

Saumande J, Chupin D. Induction of superovulation in cyclic heifers: the inhibitory effect of large doses of PMSG. *Theriogenology* 1986;**25**:233–247.

Schramm RD, Al-Sharhan M. Fertilization and early embryology: development of in-vitro-fertilized primate embryos into blastocysts in a chemically defined, protein-free culture medium. *Hum Reprod* 1996;**11**:1690–1697.

Seshagiri PB, Bavister BD. Phosphate is required for inhibition by glucose of development of hamster 8-cell embryos in vitro. *Biol Reprod* 1989;**40**:607–614.

Severini C, Ciotti MT, Biondini L, Quaresima S, Rinaldi AM, Levi A, Frank C, Possenti R. TLQP-21, a neuroendocrine VGF-derived peptide, prevents cerebellar granule cells death induced by serum and potassium deprivation. *J Neurochem* 2007;**104**:534–544.

Simurda T, Brunclikova M, Asselta R, Caccia S, Zolkova J, Kolkova Z, Loderer D, Skornova I, Hudecek J, Lasabova Z *et al.* Genetic variants in the FGB and FGG genes mapping in the beta and gamma nodules of the fibrinogen molecule in congenital quantitative fibrinogen disorders associated with a thrombotic phenotype. *Int J Mol Sci* 2020;**21**:4616.

Soto-Heras S, Paramio M-T, Thompson JG. Effect of pre-maturation with C-type natriuretic peptide and 3-isobutyl-1-methylxanthine on cumulus-oocyte communication and oocyte developmental competence in cattle. *Anim Reprod Sci* 2019;**202**:49–57.

Sterrenburg MD, Veltman-Verhulst SM, Eijkemans MJ, Hughes EG, Macklon NS, Broekmans FJ, Fauser BC. Clinical outcomes in relation to the daily dose of recombinant follicle-stimulating hormone for ovarian stimulation in in vitro fertilization in presumed normal responders younger than 39 years: a meta-analysis. *Hum Reprod Update* 2011;**17**:184–196.

Sugano M, Watanabe S. Use of highly purified porcine FSH preparation for superovulation in Japanese black cattle. *J Vet Med Sci* 1997;**59**:223–225.

Vander Ark A, Cao J, Li X. TGF-β receptors: in and beyond TGF-β signaling. *Cell Signal* 2018;**52**:112–120.

Varani S, Elvin JA, Yan C, DeMayo J, DeMayo FJ, Horton HF, Byrne MC, Matzuk MM. Knockout of pentraxin 3, a downstream target of growth differentiation factor-9, causes female subfertility. *Mol Endocrinol* 2002;**16**:1154–1167.

Ward FA, Lonergan P, Enright BP, Boland MP. Factors affecting recovery and quality of oocytes for bovine embryo production

in vitro using ovum pick-up technology. *Theriogenology* 2000;**54**: 433–446.

Yang M, Tao J, Chai M, Wu H, Wang J, Li G, He C, Xie L, Ji P, Dai Y *et al.* Melatonin improves the quality of inferior bovine oocytes and promoted their subsequent IVF embryo development: mechanisms and results. *Molecules* 2017;**22**:2059.

Yoshimura Y, Nagamatsu S, Ando M, Iwashita M, Oda T, Katsumata Y, Shiokawa S, Nakamura Y. Insulin-like growth factor binding protein-3 inhibits gonadotropin-induced ovulation, oocyte maturation, and steroidogenesis in rabbit ovary. *Endocrinology* 1996;**137**:438–446.

Yu B-Y, Subudeng G, Du C-G, Liu Z-H, Zhao Y-F, Namei E, Bai Y, Yang B-X, Li H-J. Plasminogen activator, tissue type regulates germinal

vesicle breakdown and cumulus expansion of bovine cumulus-oocyte complex in vitro. *Biol Reprod* 2019;**100**:1473–1481.

Zhai Y, Yao G, Rao F, Wang Y, Song X, Sun F. Excessive nerve growth factor impairs bidirectional communication between the oocyte and cumulus cells resulting in reduced oocyte competence. *Reprod Biol Endocrinol* 2018;**16**:28.

Zhang L, Feng T, Spicer LJ. The role of tight junction proteins in ovarian follicular development and ovarian cancer. *Reproduction* 2018; **155**:R183–R198.

Zhou X, Hao Q, Liao P, Luo S, Zhang M, Hu G, Liu H, Zhang Y, Cao B, Baddoo M *et al.* Nerve growth factor receptor negates the tumor suppressor p53 as a feedback regulator. *Elife* 2016;**5**:e15099.